Synthesis and Characterizations of Mesoporous YVO_4: Eu^{3+}@SiO_2

To cite this article: S W Li and Y F Liu 2019 *IOP Conf. Ser.: Mater. Sci. Eng.* **479** 012118

Synthesis and Characterizations of Mesoporous YVO_4: Eu^{3+}@SiO_2

S W Li[1] and Y F Liu

College of Science, Changchun Institute of Technology, Changchun 130012, China

[1] E-mail: lx_lsw@ccit.edu.cn

Abstract. The mesoporous YVO_4: Eu^{3+}@SiO_2 was synthetized by combination of in-situ synthesis with soft template method. At the same time, the mesoporous SiO_2 and YVO_4: Eu^{3+} nanocrystal were also synthesized. The structure, morphologies, UV – vis spectra, photoluminescence properties and fluorescence lifetimes were studied systemically. And the photoluminescence property of mesoporous YVO_4: Eu^{3+}@SiO_2 was studied comparing with YVO_4: Eu^{3+} nanocrystal. The results showed that the mesoporous YVO_4: Eu^{3+}@SiO_2 possessed highly ordered mesoporous structure. The intrinsic excitation bands of Eu^{3+} disappear. Under excited VO_4^{3+}, the characteristic emission of Eu^{3+} ions was obtained in the mesoporous YVO_4: Eu^{3+}@SiO_2. The lifetimes of Eu^{3+} become short in the mesoporous YVO_4: Eu^{3+}@SiO_2. The photoluminescence efficiency of mesoporous YVO_4: Eu^{3+}@SiO_2 was higher than that of the YVO_4: Eu^{3+} nanocrystal.

1. Introduction

Lanthanide ions doped materials have attracted significant attention due to their unique luminescent properties and their potential applications in laser materials, flat panel display, cathode ray tubes, up- or down- conversion materials, biomarkers and so on [1-4]. YVO_4 has been widely used as a host lattice for lanthanide ions to produce phosphors emitting a variety of colors [5-8]. YVO_4:Eu^{3+} material has higher thermal stability and is considered as the efficient red emission phosphor used in cathode ray tube and field emission display devices [5-8]. YVO_4:Eu^{3+} has the strong red emission lines ($^5D_0$-$^7F_2$ emission transitions at 614 and 619 nm) by the energy transfer to Eu^{3+} ion following absorption of UV light in the VO_4^{3-} group. YVO_4: Eu^{3+} phosphors are attracting the attention for application to field emission display (FED) devices due to its sulfur-free composition and fabrication of thin film in relatively low temperature [9, 10]. Mesoporous material has nanosize pores whose size in the range 2 – 50 nm in structure has been expected for applications of adsorbent, catalyst carrier, separation membrane, fixing agent for biomolecule and semiconductor cluster, functional electronics and photonics materials [11-13]. Especially, mesoporous silica had been studied widely in the mesoporous materials [14-16]. Mesoporous silica are highly ordered mesoporous molecular sieve with a hexagonal array of uniform channels. They have a huge specific surface area more than 1000 m^2/g and range of relatively uniform pore size from 1 to 2 nm. It has been numerous studied about mesoporous silica because of increasing need in expectations for new applications such as adsorbent and catalyst carrier. However, the photoluminescence mesoporous silica is studied rarely [17]. In this paper, we synthetized mesoporous YVO_4: Eu^{3+}@SiO_2 materials through the combination of in- situ synthesis with soft template method. The structure, morphology and luminescent properties were studied in detail.

2. Experiments sections

The preparation of YVO_4: Eu^{3+} precursor solution: weighing suitable amount of Y_2O_3 and Eu_2O_3 (mole ratio of 95:5), adding suitable amount of glacial acetic acid, heating and stirring until it completely dissolved, continue heating until excess acetic acid solution boiled away. Taking 0.112 g of above rare earth acetate and dissolving in 30 ml deionized water, forming acetic acid rare earth salt aqueous solution. Adding 0.125 g of $Na_3VO_4 \cdot 12H_2O$ into the rare earth acetate solution, strong stirring for 2 h. Weighing proper amount of CTAB dissolved in 40 ml of deionized water, then adding 5 ml of TEOS into it under stirring for 2 h. The YVO_4: Eu^{3+} precursor solution is added dropwisely into the TEOS aqueous solution with CTAB. Then the mixing solution was transferred into a Teflon bottle held in a stainless steel autoclave, sealed, and maintained at 100 °C for 48 h. The autoclave was cooled to room temperature naturally. The precipitates were separated by centrifugation, washed three times with deionized water, and dried in air at 75 °C for 24 h. Then dried product was put into the temperature control furnace at 550 ^oC for 3 h. The resulting product is marked as YVO_4: Eu^{3+}@SiO_2. As a control, we synthetized YVO_4: Eu^{3+} nanocrystal according reference [18]. And the mesoporous SiO_2 synthetized in accordance with the above methods of mesoporous YVO_4: Eu^{3+}@SiO_2.

X-ray powder diffraction (XRD) was tested on Bruker D8 Focus diffractometer (Cu-Kα as the radiation source ($\lambda = 0.15405$ nm). Transmission electron microscopic (TEM) image was taken with a FEI Tecnai G2 S-Twin. The photoluminescence spectra were obtained by a Hitachi F – 7000 spectrophotometer equipped with a 150 W xenon lamp as the excitation source. Ultraviolet-visible absorption spectra were taken with the U – 3310 scanning spectrophotometer. The decay curves were obtained via a Lecroy Wave Runner 6100 Digital Oscilloscope (1 GHz).

3. Results and discussions

3.1. structure

Figure 1A showed the Wide-angle XRD image of mesoporous SiO_2, YVO_4: Eu^{3+}@SiO_2 and YVO_4: Eu^{3+} nanocrystal. It is clearly that three peaks of diffraction were found in the mesoporous YVO_4: Eu^{3+}@SiO_2, which matching with the four corners of the YVO_4 (2, 0, 0), (1, 1, 2), (1 2 3) (JCPDS No. 76-1649), besides the broad peak of mesoporous SiO_2 (JCPDS 29-0085). It indicated that YVO_4 crystal structure is formed in the mesoporous structure. The average size of YVO_4: Eu^{3+} nanocrystal was estimated from Schereer formula, $D = K\lambda/\beta\cos\theta$, where D is the average size of particles, K is a constant (0.89), λ is X-ray wavelength (0.15405 nm), β is full width at half maximum, θ is the corresponding angle of diffraction peak, respectively. The results showed that the average size of YVO_4: Eu^{3+} nanocrystal about 0.8 nm, which is smaller than the thickness of the pore wall (~ 1.5 nm). It suggested that YVO_4 nanoparticles are formed in the mesoporous pore wall. Figure 1B showed Low angle XRD patterns of mesoporous SiO_2 and YVO_4: Eu^{3+}@SiO_2. In the mesoporous YVO_4: Eu^{3+}@SiO_2, three characteristic peaks (100), (110) and (200) could be clearly observed, which are similar to that of mesoporous SiO_2. It suggested mesoporous YVO_4: Eu^{3+}@SiO_2 still had highly ordered two-dimensional hexagonal symmetric mesoporous structure.

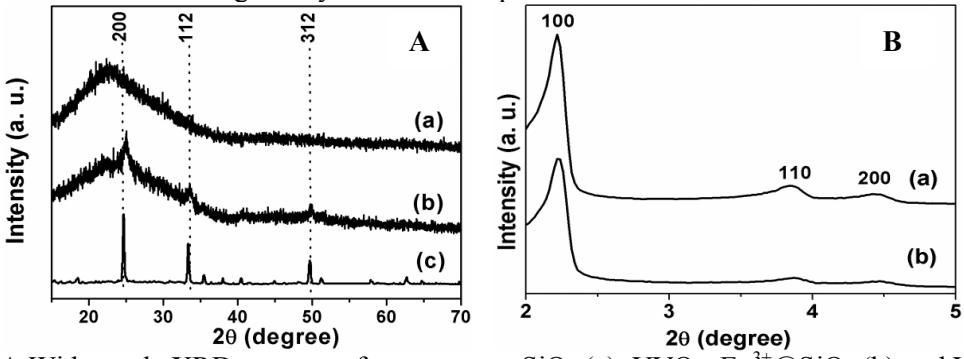

Figure 1. A Wide-angle XRD patterns of mesoporous SiO_2 (a), YVO_4: Eu^{3+}@SiO_2 (b) and YVO_4:Eu^{3+} nanocrystal (c); **B** Low-angle XRD patterns of mesoporous SiO_2 (a) and YVO_4: Eu^{3+}@SiO_2 (b).

3.2. morphologies

Figure 2(a) and (b) showed the TEM of mesoporous SiO_2 and mesoporous YVO_4: Eu^{3+}@SiO_2, respectively. Figure 2(a) show that the mesoporous SiO_2 have regular hexagonal mesoporous structure. The YVO_4: Eu^{3+}@SiO_2 (Figure 2(b)) is similar to the mesoporous SiO_2. We did not find the single nanoparticle or other structure in the all TEM of YVO_4: Eu^{3+}@SiO_2. The selected area electron diffraction patterns (SAED) of YVO_4: Eu^{3+}@SiO_2 is shown in the illustration of Figure 2(b) and the crystal diffraction rings are clearly. The results and the results of XRD can prove that the YVO_4: Eu^{3+}@SiO_2 mesoporous structure is formed.

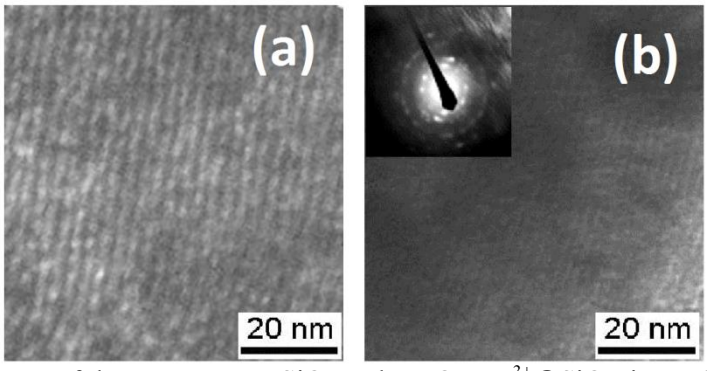

Figure 2. TEM of the mesoporous SiO_2 and YVO_4: Eu^{3+}@SiO_2, inset: SAED.

3.3. UV-vis absorption spectra

The UV-vis absorption spectra of YVO_4: Eu^{3+} nanocrystal and mesoporous YVO_4: Eu^{3+}@SiO_2 drawn in Figure 3. The shapes of UV-vis absorption spectra in both YVO_4: Eu^{3+} nanocrystal and mesoporous YVO_4: Eu^{3+}@SiO_2 are similar. In YVO_4: Eu^{3+} nanocrystal, the absorption band located around 285 nm can be observed, corresponding to the absorption of VO_4^{3+}. The clearly blue-shifts are detected for the bands in the mesoporous YVO_4: Eu^{3+}@SiO_2 samples, which can be attributed to the interaction of VO_4^{3+} with the grids Si-O-Si.

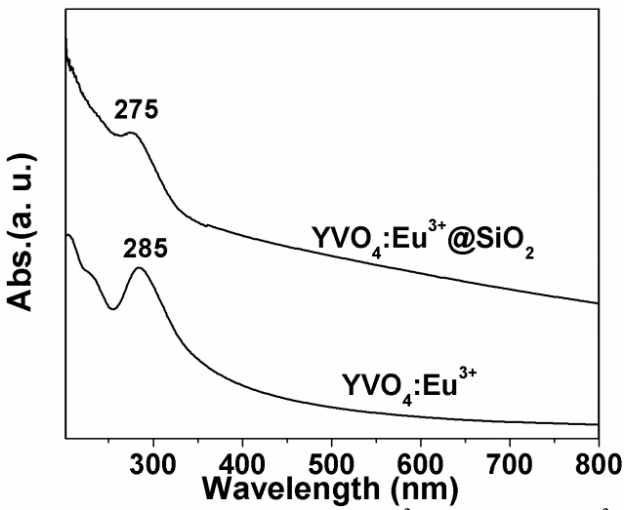

Figure 3. UV-vis absorption Spectra of the YVO_4:Eu^{3+} and YVO_4: Eu^{3+}@SiO_2.

3.4. Photoluminescence properties

The photoluminescence spectra of YVO_4: Eu^{3+} nanocrystal and mesoporous YVO_4: Eu^{3+}@SiO_2 were shown in Figure 4. In the excitation spectra (at left of Figure 4), the excitation band centered at 283 nm is attributed to the charge transfer from coordination oxygen to vanadium atom of VO_4^{3-} in YVO_4:

Eu^{3+}. Compared with YVO_4: Eu^{3+} nanocrystal, the excitation band of YVO_4: Eu^{3+}@SiO_2 becomes narrowed and the intrinsic excitation bands of Eu^{3+} at 394 nm and 456 nm disappeared, which implied that the local environment of Eu^{3+} changed. In the emission spectrum (at right of Figure 4), the composition of emissions associated with the electronic transitions from excited $^5D_{0\text{-}1}$ levels to the ground $^7F_{1\text{-}4}$ levels of Eu^{3+} ions. Among them, the emission at 592 nm ($^5D_0 \rightarrow {}^7F_1$) originating from magnetic dipole transitions and the emission at 612 nm ($^5D_0 \rightarrow {}^7F_2$) originating from electric dipole transitions are very remarkable. The shape and the emission peak position of the spectra in YVO_4: Eu^{3+}@SiO_2 and YVO_4: Eu^{3+} nanocrystal are similar. However, the emission intensity of Eu^{3+} ions in YVO_4: Eu^{3+} nanocrystal is stronger. The reason can be attributed to the excellent crystallinity of YVO_4: Eu^{3+} nanocrystal, and the local environments surrounding the Eu^{3+} ions become relative order in YVO_4: Eu^{3+} nanocrystal.

The fluorescence decay curves for the $^5D_0$-$^7F_2$ transition of Eu^{3+} ions at 612 nm in YVO_4: Eu^{3+} nanocrystal and mesoporous YVO_4: Eu^{3+}@SiO_2 were measure at room temperature, and drown in Figure 5. It can be seen that the fluorescence decay curves were nonexponential. The fluorescence decay curves can be well fitted by the following equation,

$$I = I_1 \exp(-\tau_1 / t) + I_2 \exp(-\tau_2 / t)$$

where τ_1 and ccc are the faster and slower decay time constants, respectively. I_1 and I_2 present ratios of the faster and slower components, respectively. The fitted results were 746.1 μs (τ_1), 186.9 μs (τ_2) for YVO_4: Eu^{3+}, 535.2 μs (τ_1) and 90.3 μs (τ_2) for mesoporous YVO_4: Eu^{3+}@SiO_2. Compared the fitted result, both fast and slow decay time in mesoporous YVO_4: Eu^{3+}@SiO_2 were smallar than that of mesoporous YVO_4: Eu^{3+}. It indicated that the around Eu^{3+} had been changed. The the local environment of Eu^{3+} is changed. When YVO_4: Eu^{3+} is formed in the porous wall of mesoporous SiO_2, the -OH groups on the porous wall and the surface defects of mesoporous SiO_2 became nonradiation transition path, and the nonradiative relaxation increase and lifetime became short.

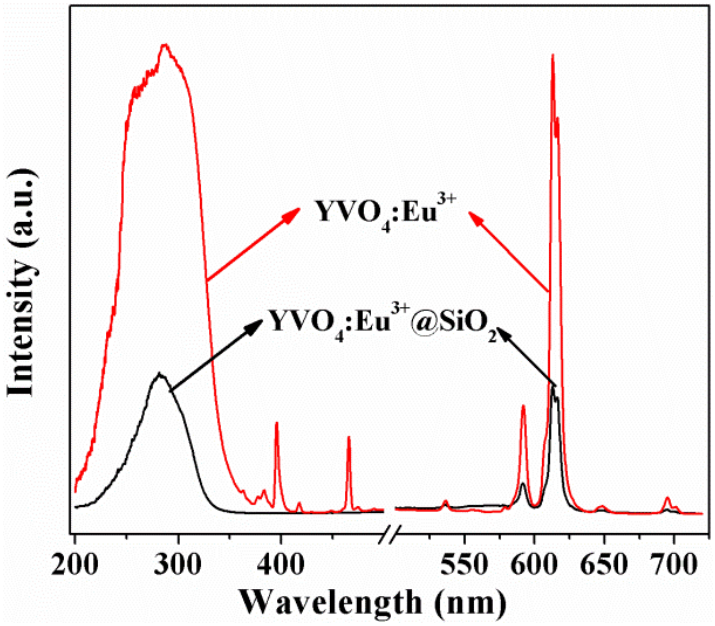

Figure 4. Excitation spectra (left) and emission spectra (right) of the YVO_4:Eu^{3+} nanocrystal and YVO_4:Eu^{3+}@SiO_2.

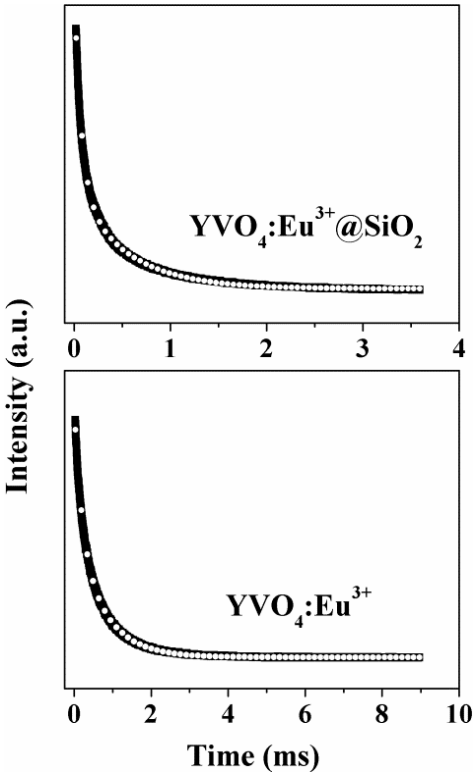

Figure 5. Fluorescent decay curves of the $^5D_0$–$^7F_2$ transitions of Eu^{3+} at 612 nm ions in YVO_4: Eu^{3+} and YVO_4: Eu^{3+}@SiO_2. The solid lines are experimental data, and the black circles are fitting functions.

4. Conclusions

Using CTAB as template, mesoporous YVO_4: Eu^{3+}@SiO_2 was prepared through in situ synthesis method. The YVO_4: Eu^{3+} nanocrystals with size about 0.8 nm were formed in the porous wall. In the mesoporous YVO_4: Eu^{3+}@SiO_2, the excitation band of vanadate becomes narrow and the intrinsic excitation bands of Eu^{3+} disappear. The characteristic luminescence of Eu^{3+} ions was obtained in the mesoporous YVO_4: Eu^{3+}@SiO_2 under excited VO_4^{3+}. The lifetimes of Eu^{3+} become short for the mesoporous YVO_4: Eu^{3+}@SiO_2. The luminescent efficiency of mesoporous YVO_4: Eu^{3+}@SiO_2 is higher than that of the YVO_4: Eu^{3+} nanocrystal.

Acknowledgements

This work was financially supported by the 13th Five-Year science and technology project of Jilin Province Education Department (Grant No. JJKH20180978KJ) and the college fund project of Changchun Institute of Technology (320180026).

References

[1] Zheng W, Huang P, Tu D T, Ma E, Zhu H M and Chen X Y 2015 *Chem. Soc. Rev.* **44** 1379-1415
[2] Yan B, Su X Q and Zhou K 2006 *Mater. Res. Bull.* **41** 134
[3] Wang F, Deng R R and Liu X G 2014 *Nature protocols* **9** 1634-1644
[4] Li S W, Huang Q Q, Jiang Y and Hu M 2016 *J. Nanosci. Nanotech.* **16** 3679-83
[5] Wang F, Liu C, Zhou Z, Jia P and Lin J 2012 *J. Rare Earths* **30** 202-2010
[6] Rambabu U, Munirathnam N R, Chatterjee S, Reddy B S and Sang-Do Han 2013 *Ceram. Int.* **39** 4801-4811
[7] Yu M, Lin J and Fang J. 2005 *Chem. Mater.* **17** 1783-91
[8] Sun Y J, Liu H J, Wang X, Kong X G and Zhang H. 2006 Chem. Mater. **18** 2726-32
[9] Wang F, Xue X and Liu X 2008 *Angew. Chem. Int. Ed.* **47** 906-9011
[10] RobindroSingh L 2017 *OpenNano* **2** 57-63

[11] Zhang L L, Xing Z P, Zhang H, Li Z Z, Wu X Y, Zhang X D, Zhang Y and Zhou W 2016 *Appl. Catal. B* **180** 521-529
[12] Wu X L, Shi Y, Zhong S, Lin H and Chen J R 2016 *Appl. Surf. sci.* **378** 80-86
[13] Wang Z, Zhu H B, Cao N, Du R K, Liu Y Q and Zhao G Z 2017 *Mater. Lett.* **186** 274-278
[14] Zhou X and Shi T J 2012 *Appl. Surf. Sci.* **259** 566-573
[15] Yu X, Chen S, Yan K, Cai X, Hu H w, M Peng, Chen B X, Dong B, Gao X and Zou D C 2016 *J. Power Sources* **325** 534-540
[16] Jin B B, He J H, Yao L, Zhang Y and Li J 2017 *ACS appl. mater.* **9** 17466-17475
[17] Zhang J, Wang Y H, xu Z G, Zhang H X, Dong P Y, Guo L N, Li F H, Xin S Y and Zheng W 2013 *J. Mater. Chem. B* **1** 330-338
[18] Huang H Y, Yang R T and Chinn D 2003 *Ind. Eng. Chem. Res* **42** 2427